J Mater Sci: Mater Med (2009) 20:1475–1481
DOI 10.1007/s10856-009-3700-x

Designer self-assembling peptide scaffold stimulates pre-osteoblast attachment, spreading and proliferation

Feng Zhang · Geng-Sheng Shi · Ling-Fei Ren · Fei-Qing Hu · Sheng-Lai Li · Zhi-Jian Xie

Received: 19 November 2008 / Accepted: 22 January 2009 / Published online: 13 February 2009

Abstract A new peptide scaffold was made by mixing pure RADA16 (Ac-RADARADARADARADA-CONH2) and designer peptide RGDA16 (Ac-RADARGDARADAR GDA-CONH2) solutions, and investigate any effect on attachment, spreading and proliferation of pre-osteoblast (MC3T3-E1). The peptides, RADA16 and RGDA16, were custom-synthesized. They were solubilized in deionized water at a concentration of 10 mg/ml (1% w/v), the RGDA16 peptide solution was mixed 1:1 with RADA16 solution and a new peptide solution RGDAmix was produced. The RGDAmix and RADA16 solution were directly loaded in 96-well plates and cover slips, and two different peptide scaffolds were formed with the addition of maintenance medium (α-MEM) in several minutes. About 1.0×10^4 MC3T3-E1 cells were seeded on each hydrogel scaffold, and then the cell morphological changes were observed using a fluorescence microscope at 1 h, 3 h and 24 h timepoint, respectively. Cell attachment was evaluated 1 h, 3 h and 24 h after cell seeding and cell proliferation was determined 4d, 7d and 14d after cell seeding. The RGDAmix scaffold significantly promoted the initial cell attachment compared with the RADA16 scaffold. MC3T3-E1 cells adhered and spread well on both scaffolds, however, cells spread better on the RGDAmix scaffold than on the RADA16 scaffold. Cell proliferation was greatly stimulated when cultured on RGDAmix scaffold. The RGD sequence contained peptide scaffold RGDAmix significantly enhances MC3T3-E1 cells attachment, spreading and proliferation.

F. Zhang · F.-Q. Hu · S.-L. Li · Z.-J. Xie (✉)
Department of Oral and Maxillofacial Surgery, The Affiliated Stomatology Hospital, College of Medicine, Zhejiang University, 395# Yan'an Road, Hangzhou 310006, People's Republic of China
e-mail: xzj66@zju.edu.cn; painfulzf@yahoo.cn

G.-S. Shi · L.-F. Ren
Taizhou Hospital of Zhejiang Province, Linhai, People's Republic of China

1 Introduction

A new class of self-assembling peptide nanofiber scaffolds has been investigated for cell culture and tissue repair [1–8]. These peptides are able to spontaneous assembly into stable hydrogels at 0.1–1% peptide concentrations. The formed scaffolds consist of greater than 99% water content, ~10 nm in fiber diameter with pores between 5 and 200 nm [1, 2]. These peptide scaffolds have three-dimensional nanofiber structure that mimic natural extracellular matrix (ECM). Self-assembling peptide scaffolds are biodegradable in the body with superior tissue biocompatibility. They have an advantage that they can be manufactured by a conventional, commercial chemical peptide synthesis method. So, their ingredients can be controlled, and they show little immunological rejection [9].

One of the self-assembling peptide scaffolds RADA16 (Ac-RADARADARADARADA-CONH2), also called PuraMatrix, has been widely investigated [2–4, 8–13]. Previous studies have shown that it could support adult mouse neural stem cells attachment, survival, proliferation and differentiation [5], enhance osteoblast proliferation, differentiation and 3-dimensional migration [6], and when mixed with other porous polymer scaffolds, the peptide scaffolds promoted osteoblast growth and differentiation [12].

Arg-Gly-Asp (RGD) is one of the most widely recognized cell adhesive motifs. RGD, first discovered by Pierchbacher [14], is found in proteins throughout the body including many bone ECM such as fibronectin, laminin,

collagen, vitronectin and so on [15, 16]. Integrin, a heterodimeric cell membrane receptor, can recognize the RGD sequence. Many studies have shown that the RGD could enhance osteoblast adhesion and spreading by combination the integrins with RGD [17–19].

The peptide PuraMatrix has motif RAD that is similar to the ubiquitous integrin receptor-binding site RGD. It is natural to design a RGD sequence containing peptide Ac-RADARGDARADARGDA-CONH2 (RDGA16) by replacing D with G in two locations. Unfortunately, when the designer peptide was solubilized in water at a concentration of 10 mg/ml (1% w/v), it remained as a non-viscous solution. However, a hydrogel was able to form when this peptide solution was mixed 1:1 with PuraMatrix solution (1% w/v). PuraMatrix can also form a hydrogel at the concentration of 0.5% (w/v), and it is difficult to distinguish whether the formed hydrogel is a new hydrogel or the hydrogel is formed only by PuraMatrix solution. In order to identify the hydrogel, an extra experiment was performed. One mg of peptide RADA16 as well and one mg RGDA16 were mixed together and the two mg peptide mixture was dissolved in 200 μl deionized water, the hydrogel was then put into a lyophilizer for one week. The weight of the total desiccated gel was about 2 mg, and this proved that hydrogel formed by mixing two peptide solutions was a new hydrogel (RGDAmix).

In the present study, we examined the initial attachment, the subsequent spreading and proliferation of mouse osteoblast-like cells (MC3T3-E1) on hydrogel scaffolds RADA16 and RGDAmix. Our observations showed the designer peptide scaffold RGDAmix promoted cell attachment, spreading and proliferation.

2 Materials and methods

2.1 Materials

RADA16 and RGDA16 peptides were custom synthesized by, and purchased from Shanghai Biotechnology Corporation, China. They were dissolved in deionized water at a final concentration of 1% (w/v) and sonicated for 30 s. The RADA16 and RGDA16 solutions were then mixed 1:1, we named this mixture RGDAmix. The RADA16 solution and RGDAmix solution were directly loaded in 96-well culture plates (Corning, USA). Maintenance medium α-MEM was added to induce hydrogel formation. These two peptide solutions were loaded on cover slips when they were sent for SEM examination and cell morphology observation.

2.2 Cell culture and seeding

Mouse pre-osteoblast cell line MC3T3-E1 (subclone 4) was purchased for this study (Cellbank of Chinese Science Academy, China). Cells were maintained in α-modified minimum essential medium (α-MEM, Gibco, USA) supplemented with 10% fetal bovine serum (FBS, Gibco, USA) at 37°C in an atmosphere with 95% humidity and 5% CO_2. The medium was replaced every 3 days and confluent cells were subcultured through trypsinization.

The scaffolds 1% (w/v) were prepared as pure RADA16 and RGDAmix. Each of the solution was sonicated for 30 s and loaded (50 μl) in the bottom of 96-well culture plates or on the center of cover slips; 50 μl α-MEM was gently added on the top of the scaffold to induce gelation. The hydrogel formed in several minutes, and rinsed twice with α-MEM to wash away any residual acidic residues remaining from peptide synthesis. Then the hydrogel was incubated in a cell culture incubator at 37°C with 5% CO_2 until cell seeding time.

Cells were seeded at 1.0×10^4 cells on the hydrogels in 96-well culture plates or on cover slips. The cells were cultured in the maintenance medium, and harvested at planned time points for analysis.

2.3 SEM sample preparation and imaging

The hydrogels, with or without cells cultured on them, were fixed in 2% glutaraldehyde at 4°C for 2 h, followed by washing with deionized water and slow sequential dehydration steps in 10% increments of ethanol for 5 min each. Samples were then placed in pressurized liquid CO_2/siphon for 1 h using a CO_2 critical point dryer. Hydrogels were next mounted, sputter coated with gold and examined by emission scanning electron microscopy (SEM, FEI, SIRION100).

2.4 Cell morphology observation

Cells cultured on the hydrogel scaffolds were washed with warm (37°C) phosphate buffer saline (PBS) and fixed in 4% paraformaldehyde/PBS at 4°C for 30 min. After three washings with PBS, the cultures were permeabilized using 0.1% Triton X-100 (Sigma, St. Louis, MO, USA) for 3 min. Then the cultures were washed twice with PBS and unspecific binding blocked with 0.5% BSA (Shanghai Sangon Biological Engineering Technology & Services Co, Shanghai, China) for another three min. Finally the cultures were incubated with 5 μg/ml rhodamine phalloidin (Sigma, USA) at 37°C for 50 min, followed by incubation with 50 μg/ml propidium iodide (Sigma, USA) at 37°C for five min. The treated cultures were washed with PBS three more times in order to remove residual dye. The cultured cell scaffolds were then observed by fluorescence microscope (Nikon, eclipse-80i, Japan). Ten random images of each sample were taken for each sample, and more than 30 single cells were randomly chosen to assess cell morphology. All images were analyzed with Image-pro plus

software (Image-pro plus 4, Media Cybernetics, Inc., Bethesda, MD, USA).

Cell morphology was described by measuring the footprint area of the cell on the hydrogel surface after attachment and using a shape factor [20, 21]. The shape factor Φ was expressed as the following:

$$\Phi = 4\pi A/P^2$$

where A is the footprint area and P is the perimeter of a cell. Circular objects have the greatest area-to-perimeter ratio, and a shape factor of one represents a perfect circle. On the contrary, a thin thread-like object would have the lowest shape factor approaching zero.

2.5 Cell attachment and proliferation

The ability of MC3T3-E1 cells to attach and proliferate on hydrogel scaffolds were determined by measurement of total DNA content in cell layers with a PicoGreen dsDNA Quantitation Kit (Invitrogen, USA). The cell-seeded scaffolds were rinsed with PBS and recovered by Na Citrate buffer solution containing 50 mM Na Citrate and 100 mM NaCl and stored at −80°C until assay. The cells were lysed in the Na Citrate solution by three freeze thaw cycles. Twenty microliters of cell lysate (200 μl/well) was mixed with 80 μl 1 × TE buffer and DNA binding fluorescent dye solution (0.5 μl Picogreen reagent in 100 μl 1 × TE buffer). The fluorescent intensity of the mixed solution was read in a fluorescence spectrometer (Sepctra M2, Molecular, USA) at an excitation wavelength of 480 nm and emission wavelength of 520 nm against a standard curve.

2.6 Statistical analysis

Statistical analysis was carried out using the SPSS statistical software package (V11, SPSS, Inc., Chicago, IL, USA). All the results were expressed as mean and standard deviation (SD) and tested for statistical significance with Student's two-tailed t-test. $P \leq 0.05$ were considered to indicate statistical significance.

3 Results

3.1 Ultra-structure self-assembling of peptide scaffolds

To observe the ultra-structure of these two peptide scaffolds, SEM examination was performed. Figure 1 is the SEM image. There is a remarkable structural similarity of nanofibers between RADA16 (Fig. 1a1, a2) and RGDAmix (Fig. 1b1, b2). Both peptide scaffolds are composed of interwoven nanofibers, and the nanofibers are ∼10 nm in diameter with 5–200 nm pores. It appears that the nanofibers of pure RADA16 are smooth and larger in diameter, while those of RGDAmix are rough and smaller in diameter. However, the surface of RGDAmix peptide scaffold seems much more irregular than that of pure RADA16 peptide scaffold.

In order to examine cell-scaffold interaction, we carried out experiments using SEM and found that cells were able to adhere and spread on the surfaces of these two peptide scaffolds (Fig. 2).

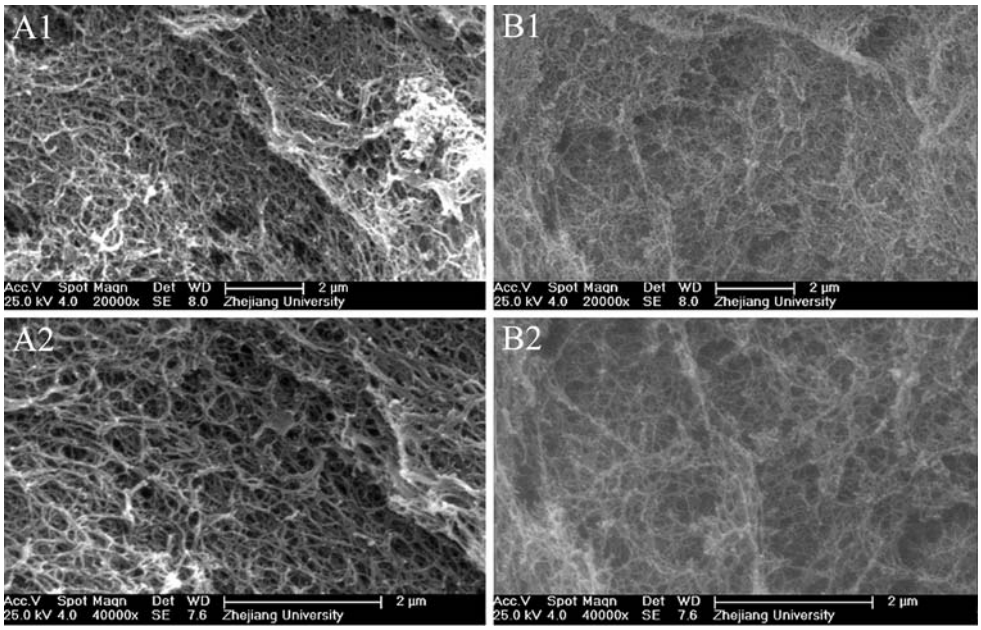

Fig. 1 SEM images of two different peptide nanofiber scaffolds. **a1**, **a2** RADA16 and **b1**, **b2** RGDAmix. The interwoven nanofibers are 10± × nm in diameter in these two peptide scaffolds with about 5–200 nm pores. Compared with RADA16, the nanofibers in RGDAmix are a little smaller in diameter and not so smooth

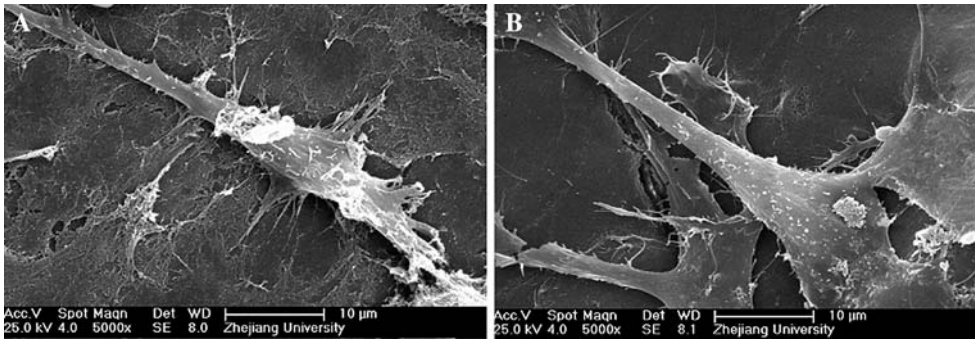

Fig. 2 SEM images of mouse MC3T3-E1 cells attached and spread with many cellular processes on the surfaces of RADA16 (**a**) and RGDAmix (**b**) peptide scaffolds

3.2 Cell morphology observation

The morphology of mouse MC3T3-E1 cells cultured on RADA16 and RGDAmix peptide scaffolds were determined by using a fluorescence microscope, and histomorphometric image analysis was performed to determine the effect of peptide scaffolds on cell attachment and spreading by measuring total cell area and cell shape factor (Fig. 3).

As it shows in Fig. 3, cells seemed to be adhering on both scaffolds with numerous pyknic cellular processes at

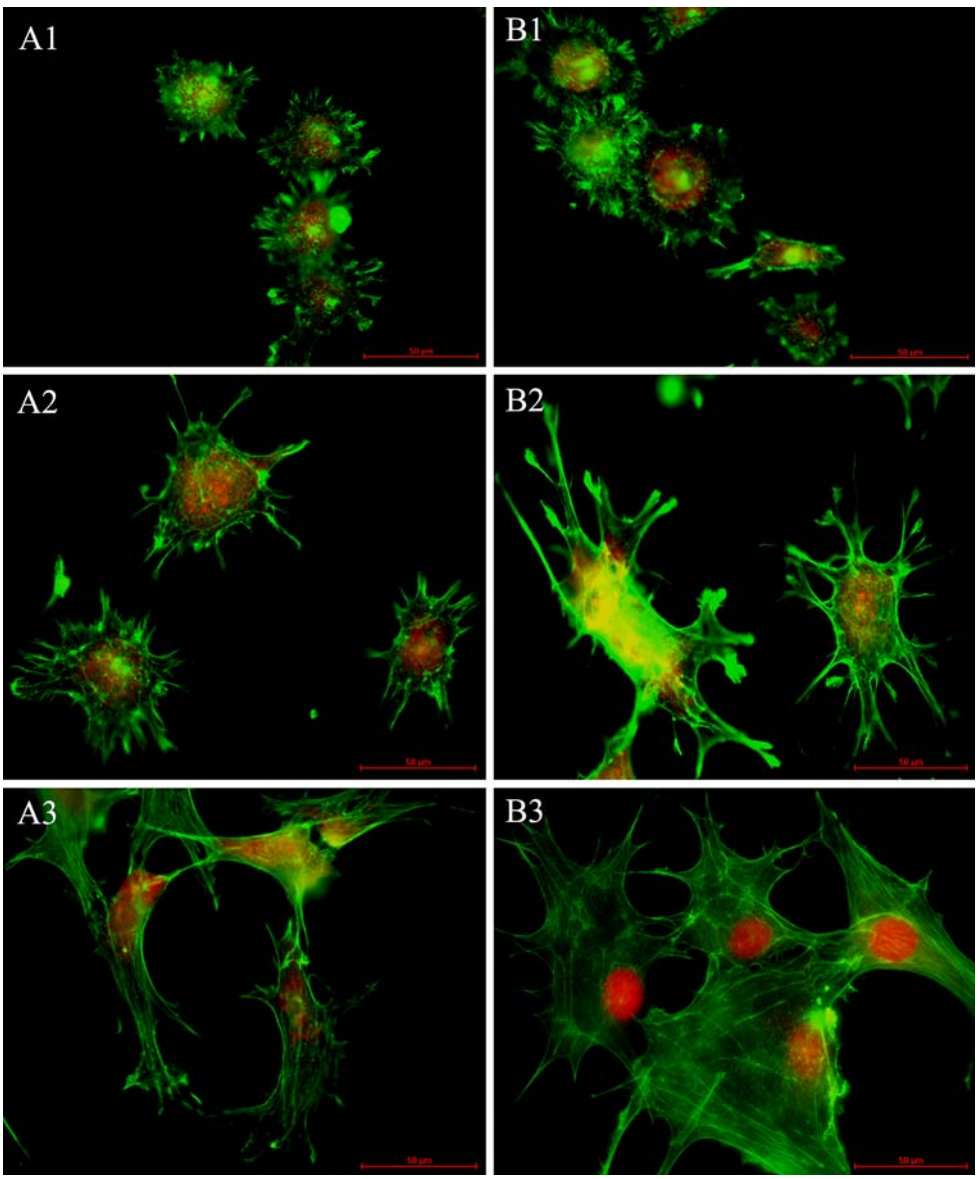

Fig. 3 Morphology of MC3T3-E1 cells cultured for 1 h, 3 h and 24 h on RADA16 and RGDAmix scaffolds. Cells were stained with rhodamine phalloidin and propidium iodide. **a** RADA16; **b** RGDAmix; **a1**, **b1** cultured for1 h; **a2**, **b2** cultured for 3 h; **a3**, **b3** cultured for 24 h. Cells cultured on RGDAmix are more elongated with numerous cellular processes compared with RADA16 scaffold (bar = 50 μm)

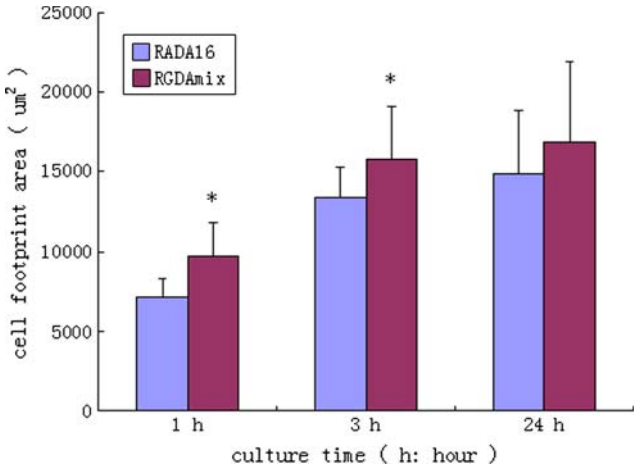

Fig. 4 Cell footprint areas are larger on RGDAmix scaffold than on RADA16 scaffold. * $P < 0.05$

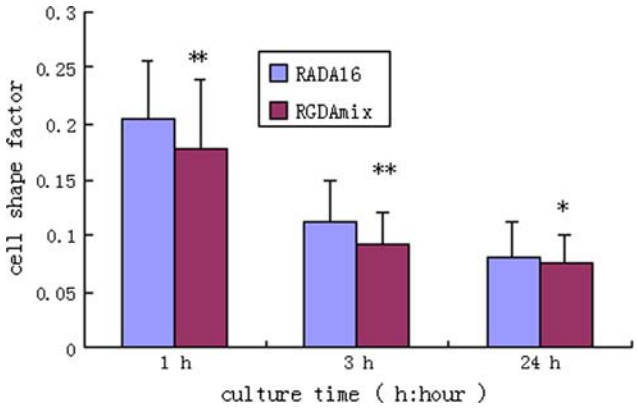

Fig. 5 Shape factor is defined as [(area/perimter^2) $\times$ 4π], and the lower the shape factor the more elongated the MC3T3-E1 cells. The cell shape factor on RADA16 scaffold is significantly higher than that on RGDAmix scaffold at all the timepoints investigated. ** $P < 0.01$; * $P < 0.05$

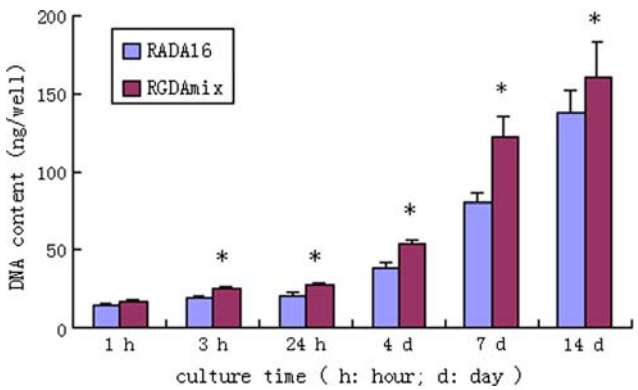

Fig. 6 Effects of peptide scaffolds on cell attachment and cell proliferation: Cell attachment and proliferation were determined by fluorescence assay. The cellular DNA content is higher on RGDAmix scaffold than on RADA16 scaffold at any timepoint. * $P < 0.05$

1 h; by 3 h, the MC3T3-E1 cells spread on both scaffolds and the cells on RGDAmix scaffold appeared showing longer and larger cellular processes. By 24 h, the cells cultured on RGDAmix scaffold were more elongated and exhibited numerous cellular processes, in contrast to the more slim morphology of MC3T3-E1 cells on RADA16 scaffold.

Footprint areas of MC3T3-E1 cells were significantly larger on RGDAmix scaffold than on RADA16 scaffold at 1 h and 3 h ($P < 0.05$; Fig. 4). At 24 h, the footprint areas of cells cultured on RGDAmix scaffold were larger than that on RADA16 scaffold without any significant difference.

As it shows in Fig. 5, the cell shape factor was very low on both peptide scaffolds at all the timepoints. However, the mean shape factor was significantly higher on RADA16 scaffold compared with RGDAmix scaffold ($P < 0.01$ or $P < 0.05$).

3.3 Cell attachment and proliferation

Figure 6 shows the mean DNA content on both scaffolds, which reflects the number of MC3T3-E1 cells attached and proliferated on RADA16 and RGDAmix scaffolds. A longer culture time resulted in a greater degree of cell attachment and proliferation. RGDAmix scaffold significantly promoted cell attachment and proliferation for all culture periods (except the time point 1 h, $P > 0.05$).

4 Discussion

A series of particular peptides have been discovered or designed, they are made from natural amino acids and can undergo self-assembly into well-ordered nanofibers and scaffolds, which show great similarity to ECM. Their assembly into nanofibers can be controlled at physiological pH simply by altering salt concentration [1, 2]. Previous studies showed these self-assembling peptide scaffolds could support cell attachment, survival and proliferation [2, 3, 13]. However, they also show great advantages over many other biomaterials. First, they are similar in scale to the native ECM and provide a suitable microenvironment. They can be broken down into natural amino acids and reused. Finally, they are synthetic and can be easily modified at the single amino acid level, and seem to be immunological inert [4, 11, 13].

In this study, we design a new peptide RGDA16, which has two-unit RGD sequence, from the peptide RADA16. Our original hypothesis was the new peptide can promote cell adhesion and proliferation because of the RGD sequence, but the designer peptide is not able to form hydrogel. A previous study showed that a peptide hydrogel

scaffold could be made by mixing pure RADA16 and designer peptide solutions [6]. We mixed the RADA16 and RGDA16 peptide solutions at a 1:1 ratio, and made a new peptide scaffold RGDAmix. Subsequent SEM examinations showed the new scaffold RGDAmix shared the similar microstructure to RADA16 and supported cell growth. We used mouse pre-osteoblast cells to evaluate peptide scaffold RGDAmix by measuring cell adhesion, spreading and proliferation, while the RADA16 was set as control group.

It was clear in our study that RGDAmix was better than RADA16 for cell culture. As it is indicated in Fig. 4, that footprint areas for MC3T3-E1 cells were much larger on RGDAmix compared with RADA16. Studies showed that cell footprint area and osteoblastic cell were correlated, and the greater the degree of cell spreading, the larger the footprint area and the greater the degree of adhesion [22]. That meant cells adhered and spread much better on RGDAmix. On the other hand, cell shape factor was much lower on RGDAmix than on RADA16. According to previous reports, we might draw the following conclusion: the lower the cell shape factor, the more elongated the cell [20, 21]. Multiple cellular extensions contributed to the increased total cellular area and elongated appearance of the cells [20]. This indicates that cells showed more cellular processes and spread better on RGDAmix than on RADA16. The results of DNA content (Fig. 6) on these two scaffolds implied that RGDAmix scaffold seems to promote MC3T3-E1 cell attachment and proliferation compared with RADA16 scaffold. Succinctly, the designer peptide scaffold RGDAmix significantly enhanced cell initial attachment, spreading and proliferation in comparison to the pure RADA16 scaffold.

The designer peptide RGDA16 has a two-unit RGD cell attachment motif for integrin receptors, and the linear or cyclic RGD are both known to promote different degrees of cell attachment and proliferation [23, 24]. Many previous studies showed modification of a hydrogel scaffold by incorporation of RGD sequence was one of the promising approaches to improve cell attachment and proliferation [25–28]. Our findings demonstrated the peptide scaffold RGDAmix stimulated cell attachment, spreading and proliferation, and it might be attributed to the RGD sequence in the peptide RGDA16.

RADA16 peptide scaffold is a promising biological material for 3-dimension cell culture, and many cell types have been studied using it [3, 4, 9–13]. The RADA16 peptide has motif RAD that is similar to the integrin receptor-binding site RGD. However, the function of motif RAD is not so definite. Some reports indicated that there was no significant difference in the cell attachment activity between the motif RGD and RAD [2, 29]. But Horii et al. [6] reported that a new peptide scaffold, which was made by extending the RADA16 at the C-terminus with RGD motif, could significantly promote pre-osteoblast proliferation and differentiation. From this report and the present study, it seems that the motif RGD plays a more important role in cell attachment, spreading and proliferation than the motif RAD.

This kind of peptide scaffolds will have a wide application in dentistry, especially the treatment of bone defects caused by periodontal disease. This kind of bone defect is usually irregular and the total volume of bone defect around a tooth is relative small. Fortunately, the peptide scaffold is highly hydrated, with more than 99% water content it can fill an irregular void before assembly and then assemble to form the molecular nanofiber scaffold. Despite the relative fragility of the peptide scaffold, it self-assembles around the tooth root and would not suffer any large external pressure. This in situ self-assembly may be critical, because most other materials do not conform to irregular voids created by inflammation or injury. The intimate contact may be critical to facilitate cell-scaffold interaction, and encouraging bone regeneration.

Acknowledgments This work was sponsored by Zhejiang Provincial Program for the Cultivation of High-level Innovative Health Talents. And supported by Grant of Health Bureau of Zhejiang Province (WKJ 2007-2-015) and Grant of Science and Technology Department of Zhejiang Province (2007C 23016), China.

References

1. S. Zhang, T. Holmes, C. Lockshin, A. Rich, Proc. Nat. Acad. Sci. USA **90**, 3334 (1993). doi:10.1073/pnas.90.8.3334
2. S. Zhang, T.C. Holmes, C.M. DiPersio, R.O. Hynes, X. Su, A. Rich, Biomaterials **16**, 1385 (1995). doi:10.1016/0142-9612(95)96874-Y
3. J. Kisiday, M. Jin, B. Kurz, H. Hung, C. Semino, S. Zhang, A.J. Grodzinsky, Proc. Nat. Acad. Sci. USA **99**, 9996 (2002). doi:10.1073/pnas.142309999
4. R.G. Ellis-Behnke, Y.X. Liang, S.W. You, D.K. Tay, S. Zhang, K.F. So, G.E. Schneider, Proc. Nat. Acad. Sci. USA **103**, 5054 (2006). doi:10.1073/pnas.0600559103
5. F. Gelain, D. Bottai, A. Vescovi, S. Zhang, PLoS ONE **1**, e119 (2006). doi:10.1371/journal.pone.0000119
6. A. Horii, X. Wang, F. Gelain, S. Zhang, PLoS ONE **2**, e190 (2007). doi:10.1371/journal.pone.0000190
7. K.M. Galler, A. Cavender, V. Yuwono, H. Dong, S. Shi, G. Schmalz, J.D. Hartgerink, R.N. D'Souza, Tissue Eng. Part A **14**, 2051 (2008). doi:10.1089/ten.tea.2007.0413
8. K. Hamada, M. Hirose, T. Yamashita, H. Ohgushi, J. Biomed. Mater. Res. A **84**, 128 (2008). doi:10.1002/jbm.a.31439
9. T.C. Holmes, S. de Lacalle, X. Su, G. Liu, A. Rich, S. Zhang, Proc. Nat. Acad. Sci. USA **97**, 6728 (2000). doi:10.1073/pnas.97.12.6728
10. D.A. Narmoneva, O. Oni, A.L. Sieminski, S. Zhang, J.P. Gertler, R.D. Kamm, R.T. Lee, Biomaterials **26**, 4837 (2005). doi:10.1016/j.biomaterials.2005.01.005
11. M.E. Davis, P.C. Hsieh, T. Takahashi, Q. Song, S. Zhang, R.D. Kamm, A.J. Grodzinsky, P. Anversa, R.T. Lee, Proc. Nat. Acad. Sci. USA **103**, 8155 (2006). doi:10.1073/pnas.0602877103

12. M.A. Bokhari, G. Akay, S. Zhang, M.A. Birch, Biomaterials **26**, 5198 (2005). doi:10.1016/j.biomaterials.2005.01.040
13. M.E. Davis, J.P. Motion, D.A. Narmoneva, T. Takahashi, D. Hakuno, R.D. Kamm, S. Zhang, R.T. Lee, Circulation **111**, 442 (2005). doi:10.1161/01.CIR.0000153847.47301.80
14. M.D. Pierschbacher, E. Ruoslahti, Nature **309**, 30 (1984). doi:10.1038/309030a0
15. B.E. Rapuano, C. Wu, D.E. MacDonald, J. Orthop. Res. **22**, 353 (2004). doi:10.1016/S0736-0266(03)00180-3
16. S. Verrier, S. Pallu, R. Bareille, A. Jonczyk, J. Meyer, M. Dard, J. Amedee, Biomaterials **23**, 585 (2002). doi:10.1016/S0142-9612(01)00145-4
17. A.R. El-Ghannam, P. Ducheyne, M. Risbud, C.S. Adams, I.M. Shapiro, D. Castner, S. Golledge, R.J. Composto, J. Biomed. Mater. Res. **68**, 615 (2004). doi:10.1002/jbm.a.20051
18. A. Rezania, C.H. Thomas, A.B. Branger, C.M. Waters, K.E. Healy, J. Biomed. Mater. Res. **37**, 9 (1997). doi:10.1002/(SICI)1097-4636(199710)37:1<9::AID-JBM2>3.0.CO;2-W
19. A.G. Secchi, V. Grigoriou, I.M. Shapiro, E.A. Cavalcanti-Adam, R.J. Composto, P. Ducheyne, C.S. Adams, J. Biomed. Mater. Res. **83**, 577 (2007). doi:10.1002/jbm.a.31007
20. A.K. Shah, R.K. Sinha, N.J. Hickok, R.S. Tuan, Bone **24**, 499 (1999). doi:10.1016/S8756-3282(99)00077-0
21. M. Schuler, G.R. Owen, D.W. Hamilton, M. de Wild, M. Textor, D.M. Brunette, S.G. Tosatti, Biomaterials **27**, 4003 (2006). doi:10.1016/j.biomaterials.2006.03.009
22. R.K. Sinha, R.S. Tuan, Bone **18**, 451 (1996). doi:10.1016/8756-3282(96)00044-0
23. H. Kumagai, M. Tajima, Y. Ueno, Y. Giga-Hama, M. Ohba, Biochem. Biophys. Res. Commun. **177**, 74 (1991). doi:10.1016/0006-291X(91)91950-H
24. W.J. Grzesik, B. Ivanov, F.A. Robey, J. Southerland, M. Yamauchi, J. Dent. Res. **77**, 1606 (1998). doi:10.1177/00220345980770080801
25. R.H. Schmedlen, K.S. Masters, J.L. West, Biomaterials **23**, 4325 (2002). doi:10.1016/S0142-9612(02)00177-1
26. J.A. Burdick, K.S. Anseth, Biomaterials **23**, 4315 (2002). doi:10.1016/S0142-9612(02)00176-X
27. H. Shin, S. Jo, A.G. Mikos, J. Biomed. Mater. Res. **61**, 169 (2002). doi:10.1002/jbm.10193
28. F. Yang, C.G. Williams, D.A. Wang, H. Lee, P.N. Manson, J. Elisseeff, Biomaterials **26**, 5991 (2005). doi:10.1016/j.biomaterials.2005.03.018
29. A.L. Prieto, G.M. Edelman, K.L. Crossin, Proc. Nat. Acad. Sci. USA **90**, 10154 (1993). doi:10.1073/pnas.90.21.10154